Ripples in epitaxial graphene on the Si-terminated SiC (0001) surface

François Varchon, Pierre Mallet, Jean-Yves Veuillen, Laurence Magaud

Ripples in epitaxial graphene on the Si-terminated SiC (0001) surface

F.Varchon, P.Mallet, J.-Y.Veuillen, and L.Magaud
Institut Néel, CNRS and UJF, BP 166,
38042 Grenoble Cedex 9 France

(Dated: April 29, 2008)

Interaction with a substrate can modify the graphene honeycomb lattice and thus alter its outstanding properties. This could be particularly true for epitaxial graphene where the carbon layers are grown from the SiC substrate. Extensive ab initio calculations supported by Scanning Tunneling Microscopy experiments demonstrate here that the substrate indeed induces a strong nanostructuration of the interface carbon layer. It generates an apparent 6x6 modulation different from the interface $6\sqrt{3}\times6\sqrt{3}R30$ symmetry used for the calculation. The top carbon layer roughly follows the interface layer morphology. This creates soft 6x6 ripples in the otherwise graphene-like honeycomb lattice. The wavelength and height of the ripples are much smaller than the one found in exfoliated graphene. Their formation mechanism also differs: They are due to the weak interaction with the interface layer and not to a roughening of the plane due to the instability of a strictly two-dimensional crystal.

PACS numbers: 81.05.Uw, 71.15.Mb, 68.37.Ef, 68.65.-k
Keywords: Graphene, Graphite, DFT, STM, SiC, Silicon carbide, Graphite thin film

I. INTRODUCTION

Since the pioneering work of Wallace in 1947 [1], many exotic properties have been suggested for graphene but they could not be checked because no samples were available. Graphene synthesis was achieved for the first time between 2004 and 2005 by three different groups [2–5]. Three years later, this material maintains its promise: the room temperature quantum Hall effect has been evidenced [6] together with large coherence length and high electronic mobility [3, 4, 7]. These basic properties hold high application potential for graphene, especially in nanoelectronics (qbits, transistors) [8]. The outstanding electronic properties [9–11], together with a high potential for application, explain why graphene is becoming the new star of condensed matter physics.

Graphene is the name given to an isolated plane of carbon atoms arranged on a honeycomb lattice. The unit cell contains two equivalent carbon atoms (named A and B). Because of this peculiar lattice, graphene electrons behave like relativistic, massless fermions and are governed by a Dirac-like equation. The band structure of graphene shows two bands with a linear dispersion. They cross at the Fermi level for neutral graphene and the crossing point is called the Dirac point. The anomalous quantum Hall effect of graphene for example is a direct consequence of this band structure.

Two methods are used to synthetize high crystalline quality samples : either from mechanical exfoliation of highly oriented pyrolitic graphite (HOPG) [3, 4] or by heating 4H or 6H SiC surfaces [5, 12, 13]. We focus here on the second system that yields large samples of graphene epitaxialy grown on a SiC substrate. This approach could enable the mass production of the graphene that would be required for future nanoelectronic needs. It has been shown to produce materials consisting of a small number of graphitic layers (FLG) to one unique graphene layer [5, 14–16].

High quality graphene is required for transport properties studies and the development of nanoelectronic applications [8]. Mastering the interface morphology is a priority for this. Indeed, Angle Resolved Photoelectron Spectroscopy (ARPES) [16–21] and transport measurements [7] have shown that the system morphology has a strong effect on the electronic structure of the FLG. The main question one has to answer is how the SiC substrate impacts graphene's particular structure. Analysis of the interface geometry requires to distinguish between the two possible hexagonal SiC surfaces. On the Si-terminated surface, the existence of a common cell ($6\sqrt{3}\times6\sqrt{3}R30$ hereafter called a 6R3) for the graphene and the substrate seems coherent with the whole set of experimental data (x-ray diffraction [22–24], Low Energy Electron Diffraction (LEED) [25–27], core level shift (CLS) [18, 20, 25, 26] and scanning tunneling microscopy (STM) [25, 27, 28]). The fact that STM images evidence a 6x6 modulation of the graphene plane instead of the 6R3 features can be explained by the morphology of the interface C buffer layer as discussed later. The C-terminated case is not so clear but no 6R3 cell seems to be present at the interface. Calculations with this geometry are given here only for direct comparison.

Ab initio calculations using a highly simplified geometry for the interface (a $\sqrt{3}\times\sqrt{3}R30$ cell, hereafter called R3) have established the buffer layer role of the first C layer that electronically decouples the graphene planes from the substrate [29, 30]. Here we address the actual interface geometry for the Si-terminated surface with a 6R3 cell. On the basis of extensive ab initio calculations supported by scanning tunneling experiments we demonstrate that the substrate has a strong effect on the first carbon layer. The structure of this interface C buffer layer derives from a honeycomb lattice that is

highly distorted because of strong covalent bonding to the substrate. The top C layer roughly follows the buffer layer morphology. This results in a 6x6 modulation superimposed on the otherwise graphene-like honeycomb lattice. The formation mechanism of these ripples differs from the free standing graphene case where the roughening of the plane has been related to the instability of a perfectly two-dimensional crystal. Their amplitude and wavelength are also much smaller than in the exfoliated graphene.

Calculations and experimental details are given in part II. The third part presents the ab initio results for both Si- and C-terminated faces, for the buffer layer and for the first actual graphene layer. STM experiments are summarized in part IV and the results are discussed in part V.

II. CALCULATION AND EXPERIMENTAL DETAILS

Ab initio calculations have been performed whithin the Density Functional Theory using the code VASP [31]. Ultra soft pseudopotentials (USPP) [32] have been used with a plane wave basis cutoff equal to 211 eV. The USPP have been extensively tested : especially, the C-short USPP was shown to correctly reproduce the band structure of graphene, of graphite and the bulk and surfaces of different SiC polytypes [29]. The Perdew and Wang [33] formulation of the General Gradient Approximation is used [34]. Brillouin zone integration is performed using the Γ point.

Two sets of calculations (with one or two C layers on SiC) were performed on both Si- and C-terminated surfaces. The first one (1310 atoms) concerns the uncovered buffer layer. Four bilayers are used to describe the SiC substrate. As a start, the first C layer is made of C atoms on a flat and complete honeycomb lattice. This accounts for the ARPES results that demonstrated the existence of a σ band skeleton for the interface C layer [20]: these bands are related to the presence of a well developed honeycomb-like lattice. All the atoms are allowed to relax except in the two lower SiC bilayers and the residual forces are lower than 0.015 eV/Å. The second set of calculations models two carbon layers on top of the SiC substrate. The previous cell with an additional graphene layer would be too large to keep a reasonable computation time and we had to restrict the cell to two SiC bilayers, the buffer layer and the graphene layer (1216 atoms). Atoms in the lower SiC bilayer and the subsequent C plane are kept fixed to bulk positions. Because of the limited number of planes used to describe the substrate, the forces could not be zeroed in these three layers, which remain strained. However, forces in the top graphene plane, in the buffer layer and in the last SiC plane could be relaxed to negligible values and the calculation that started from two flat honeycomb lattices reproduces the buffer layer geometry found with the first cell. In both calculation sets, H atoms are used to saturate the dangling bonds on the second surface.

The calculations are performed in the actual 6R3 cell with respect to SiC (or 13x13 relative to graphene) that corresponds to the interface geometry on the Si-terminated SiC. In the following, periodicity expressed with respect to SiC (graphene) will be referred to -SiC (-G) for clarity.

STM experiments were performed at room temperature, in ultra-high vacuum, using a laboratory built microscope. Graphitization of n-type (nitrogen $1x10^{18}$ cm^{-3}) 6H-SiC(0001) substrates was achieved by successive annealing into UHV, monitored by LEED and Auger spectroscopy. Experiments were done first on the buffer layer surface, and second on a mixed surface with mono- and bilayer graphene areas. The details of the growth process and the determination of the layer thickness have been discussed elsewhere [14]. We used the symmetric STM atomic contrast to identify areas corresponding to monolayer graphene. Results have been checked on two different substrates with different tips and at different temperatures.

III. AB INITIO RESULTS

A. First C layer on the Si-terminated SiC surface : the buffer layer

Fig.1a shows a large scale image of the ab initio total charge density of an uncovered buffer layer (the picture is identical when it is covered by a graphene layer). It has three main characteristics: i) An obvious apparent 6x6-SiC modulation ii) The 6R3-SiC common cell periodicity that is imposed by the calculation (dashed diamond cell in Fig1.a) iii) Low regions, separated by boundaries, that form nanograins with an unexpected local 2x2-G or R3-SiC symmetry. This gives a mosaic like structure to the buffer layer.

The 6x6-SiC modulation is very apparent (cell defined by the full line diamond in Fig.1a) because it is related to the bright spots of Fig.1a and Fig.2a. It is not a real reconstruction since it is not compatible with translational symmetry within the buffer layer : Fig.1a and Fig.2a show different local environments for the atoms in the different 6x6-SiC bright spots. It is a consequence of the mosaic-like structure of the buffer layer. The mosaic pattern is composed of grains of more or less irregular hexagonal shape, 20$\mathring{A}$ wide. They are due to the superposition of the C honeycomb and SiC lattices [25]. The two lattices do not adjust to each other. The grains (dark area) corresponds to regions where the SiC and honeycomb lattices match (in a local 2x2-G or R3-SiC symmetry) and where Si-C bonds are formed. The local 2x2-G patterns (visible as small hexagonal features in the dark regions of Fig.1a) are shifted in adjacent grains, the boundaries also accomodate for this shift. C atoms that are not in register with the substrate form no bonds with

it, as shown by the cross section, Fig.2b. They lie higher above it and form boundaries (light area).

The Fourier transform of a large charge-density map of the free buffer layer (Fig.1b) and of the buffer layer covered with a graphene layer (not shown) are identical. They are in agreement with LEED data [25–27]. Apart from the 1x1-G graphene and the 6x6-SiC spots, one remarkable feature of this FT image is the rather intense spots located about midway from the 1x1-G spots (but off-axis). These spots are also found in the FT of the STM images as shown below. They belong to the reciprocal lattice of the 6R3-SiC. Their intensity is locally enhanced (in k-space) by the presence of small grains with local 2x2-G (or R3 -SiC) symmetry. We call them 2x2-G spots in the following. Additionally, the first-order spots of the 6R3 reconstruction are vanishing at the centre of Fig.1b (although higher order spots of the 6R3 are present) [35].

The corrugation of the buffer layer is rather large with a lower to upper atom height difference close to 0.12 nm (Fig.3b). In contrast to previous models proposed for the buffer layer [25, 28], the present structure comes directly from the relaxation of a complete and flat carbon honeycomb lattice lying on top of the SiC surface and performed in the actual Si-terminated interface geometry (Fig.3a). The resulting morphology is in agreement with CLS data that evidence the existence of 2 types of C atoms within the buffer layer that are respectively bound or not bound to Si atoms of SiC [20, 25].

Ab initio band structure calculations in the 2x2-G structure [29, 30] demonstrated that the interface C layer does not have the electronic structure of graphene but acts as a buffer layer since it allows growth of subsequent C planes with graphene-like dispersion. The present calculations, performed in the actual interface geometry, support this result. It demonstrates that part of the interface layer has indeed the simple 2x2-G geometry. It also further evidences the buffer role of this first C layer since a second C layer, on top of it, presents a (wavy) graphene honeycomb lattice.

B. Graphene layer on the Si-terminated SiC surface

The total charge density on the second C plane indeed shows a honeycomb lattice (Fig.4a). This plane tends to follow the morphology of the buffer layer so that the high regions of the buffer layer generate small bumps in it (Fig.5a and 5b). This creates soft ripples with the 6x6-SiC modulation of the buffer layer. No bonds are seen (Fig.5b) between this graphene layer and the buffer layer. The ripples have an amplitude of 0.04 nm for a wavelength of 1.9 nm (Fig. 6a and 6b). Such a long wavelength modulation does not discriminate between the two basis atoms, A and B, of the honeycomb lattice. No A versus B contrast can be seen on the ab initio total charge density map in agreement with the STM images (inset Fig.9a). The Fourier transform exhibits spots related to 1x1-G and 6x6-SiC periodicity (Fig.4b).

C. The C-terminated case

We would like to stress that the geometry used here for the calculation is not the one observed on this face. In fact, the actual morphology is not known but it does not seem to involve the 6R3 structure. We have calculated the total charge density maps for the C-terminated interface in this structure to compare them to the the Si-terminated case. The supercells used for the calculations are equivalent. The same complex mosaic structure appears for the first carbon layer (Fig.7a) but the hexagonal shape of the grains seems more regular and more pronounced. The bottom of the grains corresponds to the matching zones between the buffer layer and the substrate where C-C bonds are formed. All boundary intersections give rise to bright spots so that the 6x6 modulation is not so apparent. By the way, the nanostructuration of the graphene layer also appears to be stronger (Fig.7b). Experimentally, the graphene layer seems to be flatter on the C- than on the Si-terminated face. The different behavior of the two faces might come from the strength of the substrate-C layer bonds in the 6R3-SiC cell. In the C-terminated case, covalent C-C bonds are formed. They are stronger and shorter than Si-C bonds. The lattice distorsions induced in the buffer layer and subsequently in the graphene layer are stronger. They might be so large that the 6R3 geometry is not stable.

IV. STM RESULTS ON THE SI-TERMINATED SURFACE

The peculiarities of the interface evidenced by ab initio calculations are also found in Constant Current topographic STM images of the buffer layer (Fig.8a), of the first graphene monolayer (Fig.9a) and of their respective FT (Fig.8b and 9b). The fact that the STM images and the charge density maps show the same features, and especially the 6x6 modulation, demonstrate that geometric effects dominate here and that electronic (DOS) related effects play a minor role. For the uncovered buffer layer, (the so-called nanomesh or 6R3 phase in the literature [25, 27]), a honeycomb pattern with the 6x6-SiC periodicity is experimentaly observed (Fig.8a), with hexagons of irregular shapes in accordance with the calculation (Fig.1a). Although atomic resolution is hardly achieved on this surface [14, 25, 27], the FT agrees with the 2x2-G periodicity calculated for the grains. Indeed, we find some tiny spots (circled in Fig.8b) at positions close to half the reciprocal vector of the 1x1-G lattice (k=29.5 nm^{-1}). The same spots are found on the FT of the corresponding calculated total charge shown in Fig.1b.

STM images of the first graphene layer capping the buffer layer strongly support our calculated results. A

survey of the image of Fig. 9a, recorded at sample bias -0.2V, reveals both the graphene 1x1-G honeycomb pattern and the superimposed 6x6-SiC superstructure. These features are recovered in the FT shown in Fig.9b.

We can take advantage of the sensitivity of STM to the interface states [24, 36, 37] to get new insights into the buffer layer structure capped by the graphene top-layer. At low sample bias (here -0.2V), the tip probes the π-like states of graphene, together with electronic states lying within the buffer layer or at the interface with SiC [14]. In the present case, interface states give rise to additional features in the FT of the STM image related to the buffer layer. As shown in Fig. 9b, we find a clear signature of the local 2x2-G symmetry, arising as pronounced bright spots (circle) close to the 2x2-G expected value. They correspond to the spots circled in the FT of the total charge density of the free buffer layer (Fig.1b).

V. DISCUSSION

An ab initio calculation of a free rippled graphene layer, where the atomic positions are frozen in the 6x6 positions given by the present calculations, reveals an ideal graphene-like linear dispersion. The band structure calculation of a supercell containing the graphene layer, the buffer layer and enough bilayers to correctly reproduce the substrate is unfortunately out of reach for the moment. Furthermore, the calculation of the eigenvalues on several k points along the Γ K M direction shows many low dispersion states below the Fermi level that hide the graphene linear dispersion. Unfolding this 13x13 reconstruction onto the graphene 1x1 cell turns out to be impossible in our case. Thus, contrary to Kim et al [38], we cannot draw any conclusion about the existence or not of a gap at the position of the Dirac point (that is 0.4 eV below the Fermi level). In any case, although the buffer layer geometry seems to be correctly obtained with a supercell including only two SiC bilayers, this might not be enough to get the detailed band structure needed to prove on the existence of a gap 0.25 eV wide. From our ab initio results, we can say that the induced distortion differentiates areas of the graphene layer but it does not differentiate A atoms from B atoms in each unit cell. Furthermore, a careful study of STM images of a few nm square, like the 2.5 x 2.5 nm^2 image shown in inset (Fig.9a), agrees with the previous results of ref. [14]: We do not find any detectable asymmetry between the adjacent carbon atoms of the graphene layer, and we use the symmetric contrast as a signature of the monolayer (an asymmetric contrast is found for a graphene bilayer with AB stacking). We believe that this is in contradiction with the mechanism suggested by Zhou et al [21] for a possible gap opening at the Dirac point. So, if a gap is opened in the graphene band structure because of the interaction with the buffer layer, the phenomenon involved is more complex than a uniform breaking of AB sublattice symmetry. Furthermore, ARPES [16, 20], STM [14, 25] and preliminary calculations [29, 30] have demonstrated that the buffer layer presents no π band in the vicinity of the Fermi level so that, contrary to what happens in graphite, these bands cannot be involved in differentiating the A from the B sublattice. In any case, other gap-opening mechanisms could be invoked, especially the interaction of the graphene states with the low dispersion states found below the Fermi level. We know from STM experiments that many interface states are located in this energy range [14].

The formation mechanism found here for the ripples is drastically different from the one involved in the roughening of a free standing graphene layer [39, 40]. In the latter case, the ripples were related to the instability of a strictly two-dimensional crystal while here they are formed because the graphene layer follows the morphology of the underlying buffer layer. The amplitude and wavelength also differ. Both are much smaller here. The situation is more similar to what has been found in calculations modeling graphene on SiO_2 [41] where the graphene layer was distorted by interaction with the substrate. This created holes and bumps within the plane that have been associated with electron and hole pockets. Whether the same argument could apply here is not evident since the wavelength of the ripples is much smaller. Furthermore, here the graphene layer is doped : experiments and ab initio calculations in the R3 cell found that the fermi level lies 0.4 eV above the Dirac point. This makes hole pockets creation rather unlikely. Ripples in exfoliated graphene have been used to explain the absence of weak antilocalisation. This could also be the case here. As far as we know, weak antilocalisation has only been observed on the C-terminated system [11] where the 6R3 cell does not exist and where the graphene terrasses seems to be much flatter [23].

Both theory and STM experiments demonstrate that the buffer layer geometry is essentially unchanged when it is buried below one graphene monolayer. From these results, it appears that the C buffer layer is not an intermediate sublimation phase but remains at the interface. A possible scenario for growth might proceed as follows: Si atoms sublimate, the C atoms rearrange and form the buffer layer. More Si atoms disappear, the C atoms thus freed form a new buffer layer while the former one flattens to form a graphene plane. Since the buffer layer needs to form prior to the appearance of a new graphene plane, a layer by layer growth is favoured as observed experimentally [16, 24].

VI. CONCLUSION

In conclusion, we would like to emphasize the role of the C buffer layer. It is not an intermediate sublimation phase. It is always present at the Si-terminated SiC-graphene interface and it efficiently decouples the graphene layer from the substrate. Most of the interest of the system results from the presence of this layer. It has

a mosaic structure that derives from a honeycomb lattice distorted because of C-Si bond formation. This results in the appearance of a 6x6-SiC modulation also found in STM images; while the actual common cell corresponds to a $6\sqrt{3}\times 6\sqrt{3}R30$-SiC. This layer also presents a local 2x2 symmetry (with respect to graphene) in the region where the honeycomb and the SiC lattices nearly match. This unexpected local symmetry appears in the Fourier transforms of the STM images, confirming the presence of matching zones. The existence of the buffer layer agrees with a layer by layer growth mechanism where a new buffer layer is formed at the interface while the former one evolves into a graphene layer. Weak interaction with the buffer layer creates incommensurate 6x6-SiC ripples in the otherwise graphene-like second carbon layer. This incommensurate modulation, observed in STM images also, does not break the AB symmetry. The wavelength and height of the ripples here are much smaller than in exfoliated graphene. The effect of the ripples on transport properties requires further investigation since the present calculation cannot conclude whether a gap exist at the Dirac point. The role of the low dispersion interface states has also to be considered. The possible use of the nanostructuration induced by the substrate in the graphene and buffer layers in order to create arrays of nanometric size islands also deserves further consideration.

Acknowledgement

The authors acknowledge C.Naud, D.Mayou, P.Darancet, V.Olevano, E.Conrad, C.Berger and W.de Heer for fruitful discussions. They gratefully thank R.Cox for his careful reading of the manuscript. The present work was supported by the ANR GRAPHSIC project, the CIBLE07 project and computer grants from IDRIS-CNRS and the CIMENT project.

[1] P. R.Wallace *Phys. Rev.* **71**, 622-634 (1947)
[2] K. S.Novoselov, A.K.Geim, S.V.Morozov, D.Jiang, Y.Zhang, S.V.Dubonos, I.V.Grigorieva, A.A.Firsov *Science* **306**, 666-669 (2004)
[3] K. S.Novoselov, A.K.Geim, S.V.Morozov, D.Jiang, M.I.Katsnelson, I.V.Grigorieva, S.V.Dubonos, A.A.Firsov *Nature* **438**, 197-200 (2005)
[4] Y.Zhang, Y.-W.Tan, H.L.Stormer, P.Kim *Nature* **438**, 201-204 (2005)
[5] C.Berger, Z.Song, T.Li, X.Li, A.Y.Ogbazghi, R.Feng, Z.Dai, A.N.Marchenkov, E.H.Conrad, P.N.First, W.A.de Heer *J.Phys. Chem.B* **108**, 19912-19916 (2004)
[6] K. S.Novoselov, Z.Jiang, Y.Zhang, S.V.Morozov, H.L.Stormer, U.Zeitler, J.C.Maan, G.S.Boebinger, P.Kim, A.K.Geim *Science* **315**, 1379 (2007)
[7] C.Berger, Z.Song, X.Li, X.Wu, N.Brown, C.Naud, D.Mayou, T.Li, J.Hass, A.N.Marchenkov, E.H.Conrad, P.N.First, W.A.de Heer *Science* **312**, 1191-1196 (2006)
[8] A. K.Geim and K. S.Novoselov, *Nature Mat.* **6**,183-191 (2007)
[9] S. V.Morozov, K.S.Novoselov, M.J.Katsnelson, F.Schedin, L.A.Ponomarenko, D.Jiang, A.K.Geim *Phys.Rev.Lett.* **97**,016801 (2006)
[10] T.Ando, T.Nakanishi, R.Saito *J.Phys.Soc.Jpn* **67**, 2857-2862 (1998)
[11] X.Wu, X.Li, Z.Song, C.Berger, W.A. de Heer *Phys. Rev. Lett.* **98**, 136801 (2007)
[12] A. J.Van Bommel, J.E.Crombeen and A. van Tooren, *Surf.Sci.***48**, 463-472 (1975)
[13] I.Forbeaux, J. -M.Themlin, J. -M.Debever, *Phys. Rev. B* **58**, 16396-16406 (1998)
[14] P.Mallet, F.Varchon, C.Naud, L.Magaud, C.Berger, J.-Y.Veuillen *Phys. Rev. B* **76**, 041403(R) (2007)
[15] G.M.Rutter, J.N.Crain, N.P.Guisinger, T.Li, P.N.First, J.A.Stroscio *Science* **317**, 219-222 (2007)
[16] T.Ohta, A.Bostwick, J.L.McChesney, T.Seyller, K.Horn, E.Rotenberg *Phy. Rev. Lett.* **98**, 206802 (2007)
[17] T.Ohta, A.Bostwick, T.Seyller, K.Horn, E.Rotenberg *Science* **313**, 951-954 (2006)
[18] Th.Seyller, K.V.Emtsev, K.Gao, F.Speck, L.Ley, A.Tadich, L.Broekman, J.D.Riley, R.C.G.Leckey, O.Rader, A.Varykhalov, A.M.Shikin *Surf. Sci.* **600**, 3906-3911 (2006)
[19] A.Bostwick, T.Ohta, T.Seyller, K.Horn, E.Rotenberg *Nature Phys.* **3** 36-40 (2006)
[20] E. K.Emtsev, Th.Seyller, F.Speck, L.Ley, P.Stojanov, J.D.Riley, R.G.C.Leckey *Mater. Sci. Forum* **556-557**, 525 (2007)
[21] S.Y.Zhou, G.-H.Gweon, A.V.Federov, P.N.First, W.A.de Heer, D.-H.Lee, F.Guinea, A.H.Castro Neto, A.Lanzara *Nature Mat.* **6**, 771-776 (2007)
[22] J.Hass, R.Feng, T.Li, X.Li, Z.Zong, W.A.de Heer, P.N.Fisrt, E.H.Conrad, C.A.Jeffrey, C.Berger *Appl. Phys. Lett.* **89**, 143106 (2006)
[23] J.Hass, R.Feng, J.E.Millan-Otoya, X.Li, M.Sprinkle, P.N.First, W.A.de Heer, E.H.Conrad, *Phys. Rev. B* **75**, 214109 (2007).
[24] A.Charrier, A.Coati, T.Argunova, F.Thibaudau, Y.Garreau, R.Pinchaux, I.Forbeaux, J.-M.Debever, M.Sauvage-Simkin, J.-M.Themlin *J. Appl. Phys.* **92**, 2479-2484 (2002)
[25] W.Chen, H.Xu, L.Liu, X.Gao, D.Qi, G.Peng, S.C.Tan, Y.Feng, K.P.Loh, A.T.Shen Wee *Surf. Sci.* **596**, 176-186 (2005)
[26] E.Rollings, G.-H.Gweon, S.Y.Zhou, B.S.Mun, J.L.McChesney, B.S.Hussain, A.V.Fedorov, P.N.First, W.A.de Heer, A.Lanzara *J.Phys.Chem.Sol.* **67**, 2172 (2006)
[27] F.Owman, P.Martensson, *Surf. Sci.* **369**, 126-136 (1996)
[28] M. -H.Tsai, C.S.Chang, J.D.Dow, I.S.T.Tsong *Phys. Rev. B* **45**, 1327-1332 (1992)
[29] F.Varchon, R.Feng, J.Hass, X.Li, B.Ngoc Nguyen, C.Naud, P.Mallet, J.-Y.Veuillen, C.Berger, E.H.Conrad, L.Magaud *Phys. Rev.Lett.***99**, 126805 (2007)
[30] A.Mattausch and O.Pankratov, *Phys.Rev.Lett.* **99**, 076802 (2007)
[31] G. Kresse and J. Hafner, *Phys. Rev. B* **47**, 558 (1993)
[32] G. Kresse and J. Hafner, *J.Phys. Condens. Matter* **6**, 8245 (1994)
[33] J. P. Perdew and Y. Wang, *Phys. Rev. B* **33**, 8800 (1986)

[34] The LDA is known to give a good interlayer distance in graphite while the GGA fails but this is due to an error cancellation. The GGA formulation is more efficient to describe the strong covalent bonding between the SiC substrate and the buffer layer. In the starting supercell, the graphite interlayer distance was used to position the graphene layer with respect to the buffer layer. A similar calculation by the LDA gives a similar morphology of the buffer layer [38]

[35] This is not an artifact of the FT software, since when one selects only one family of 2x2-G patches arranged in a 6R3-SiC network in the image before performing the FT, the first order 6R3-SiC spots reappear. It is therefore an intrinsic property of the image, and we believe this might be related to the spatial arrangement of the 3 families of local 2x2-G grains. First order spots of the 6R3-SiC reconstruction are also absent in FT of the STM images.

[36] G.M.Rutter, N.P.Guisinger, J.N.Crain, E.A.A.Jarvis, M.D.Stiles, T.Li, P.N.First, J.A.Stroscio, ArXiv:cond-mat/0711.2523

[37] V.W.Brar, Y.Zhang, Y.Yayon, T.Ohta, J.L.McChesney, A.Bostwick, E.Rotenberg, K.Horn, M.F.Crommie *Appl.Phys.Lett* **91**, 122102 (2007)

[38] S.Kim, J.Ihm, H.J.Choi, Y.-W. Son, Arxiv:cond-mat/0712.2897

[39] J.C.Meyer, A.K.Geim, M.I.Katsnelson, K.S.Novoselov, T.J.Booth, S.Roth, *Nature***446**, 60 (2007)

[40] A.Fasolino, J.H.Los, M.I.Katsnelson, *Nature Mat***6**, 858 (2007)

[41] M.W.C.Dharma-wardana, *J.Phys:Conden.Matter* **19**, 386228 (2007)

Figure captions

Figure 1:(color online) Buffer layer on top of the Si-terminated SiC surface. The SiC-graphene common cell is defined by the dashed line diamond cell and the incommensurate 6x6-SiC modulation by the full line diamond cell. a) Mosaic structure of the C buffer layer evidenced in this 11x11 nm^2 image of the total ab initio charge density, 0.04 nm above the upper atom. b) Fourier transform of a large scale image of the total charge density. The solid arrow points to a 1x1-G spot, the dashed arrow to a 6x6-SiC spot and the spots in the circle correspond to the local 2x2-G periodicity.

Figure 2 : (color online) total charge density of the buffer layer on SiC(001). a) total charge density in the 6R3-SiC unit cell. b) cross section of the total charge density along the line defined in a). The black dots that appear when the cross section goes through the middle of an atom are due to the use of pseudopotentials (no core electrons).

Figure 3 : (color online) atomic positions in the buffer layer, in the 6R3 cell. a) positions of the atoms in the unit cell. Si atoms in the last SiC plane are in grey (larger circles). The colour of the atoms in the buffer layer varies as a fonction of their height, ranging from blue (dark grey) close the substrate to green (medium grey) for the uppermost atoms. b) Height profile of the buffer layer atoms along the line defined in a. The line is just a guide for the eyes.

Figure 4: (color online) Graphene layer above the C buffer layer for the Si-terminated surface. a) large scale image (11x11 nm^2) of the total charge density 0.04 nm above the uppermost atom. It exhibits the characteristic 6x6-SiC periodicity (full line diamond). The 6R3-SiC common cell corresponds to the dashed line diamond. b) Fourier transform of a large scale image of the total charge density. The solid arrow points to a 1x1-G spot, the dashed arrow to a 6x6-SiC spot.

Figure 5 : (color online) total charge density. a) total charge density in the 6R3-SiC unit cell, b) cross section of the total charge density along the line defined in a). The section is not taken at the same position as in Fig.2a, to focus on the graphene layer.

Figure 6 : (color online) Atomic positions in the graphene layer, in the 6R3 cell. a) positions of the atoms in the unit cell, The C atoms in the buffer layer are in grey (light grey), the colour of the atoms in the graphene layer varies as a fonction of their height, ranging from blue (dark grey) close the buffer layer to green (medium grey) for the uppermost atoms. b) Height profile of the graphene layer atoms along the line defined in (a).

Figure 7:(color online) Morphology of the buffer layer and the top graphene layer for the C-terminated SiC surface in the 6R3 cell. a) charge density map of the interface buffer layer (8x8 nm^2), b) charge density map of the top graphene layer (8x8 nm^2). The 6R3-SiC common cell (6x6-SiC periodicity) corresponds to the dashed line (full line) diamond cell.

Figure 8: (color online) STM image and its related Fourier transform of the buffer layer on the Si-terminated surface. a) 12x12 nm^2 STM image of the buffer layer (V=-2.0 V and I=0.5 nA). This clearly shows the irregular hexagonal pattern of the 6x6 -SiC periodicity.The 6R3-SiC common cell (6x6-SiC periodicity) corresponds to the dashed line (full line) diamond cell. b) Fourier transform of image (a), with the dashed arrow pointing to a 6x6-SiC spot and with the 2x2-G spots circled.

Figure 9: (color online) STM image and its related Fourier transform of the graphene layer on the Si-terminated surface. a) 12x12 nm^2 STM image of the graphene monolayer (V=-0.2 V, I=0.1 nA) (inset 2.5x2.5 nm^2). The apparent 6x6-SiC unit cell is indicated in full line. b) Fourier transform of image (a), with the solid arrow pointing to the 1x1-G spot, the dashed arrow pointing to the 6x6-SiC spots and with the 2x2-G related spots circled.

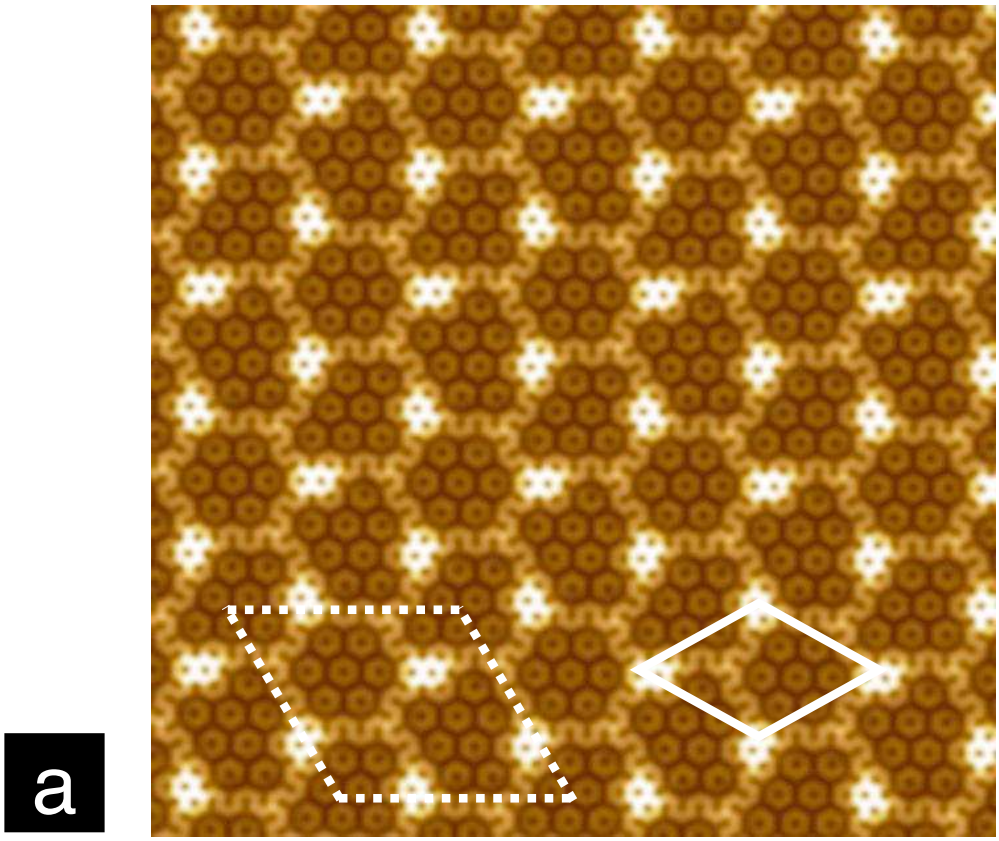

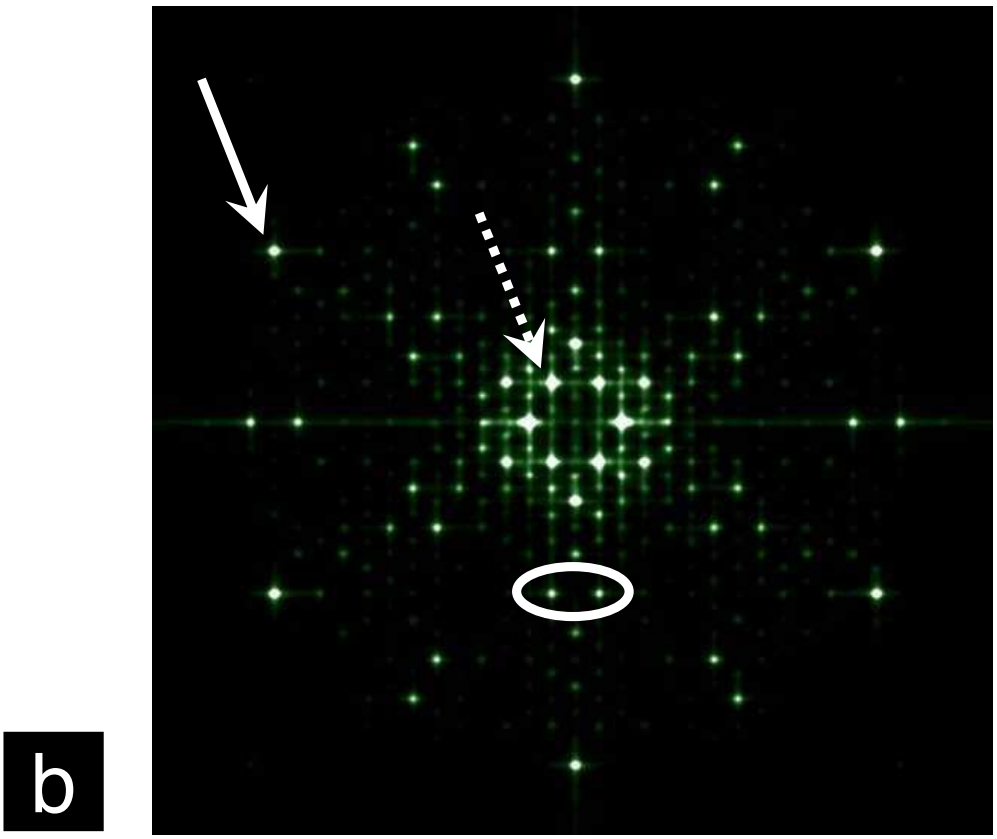

Figure 1

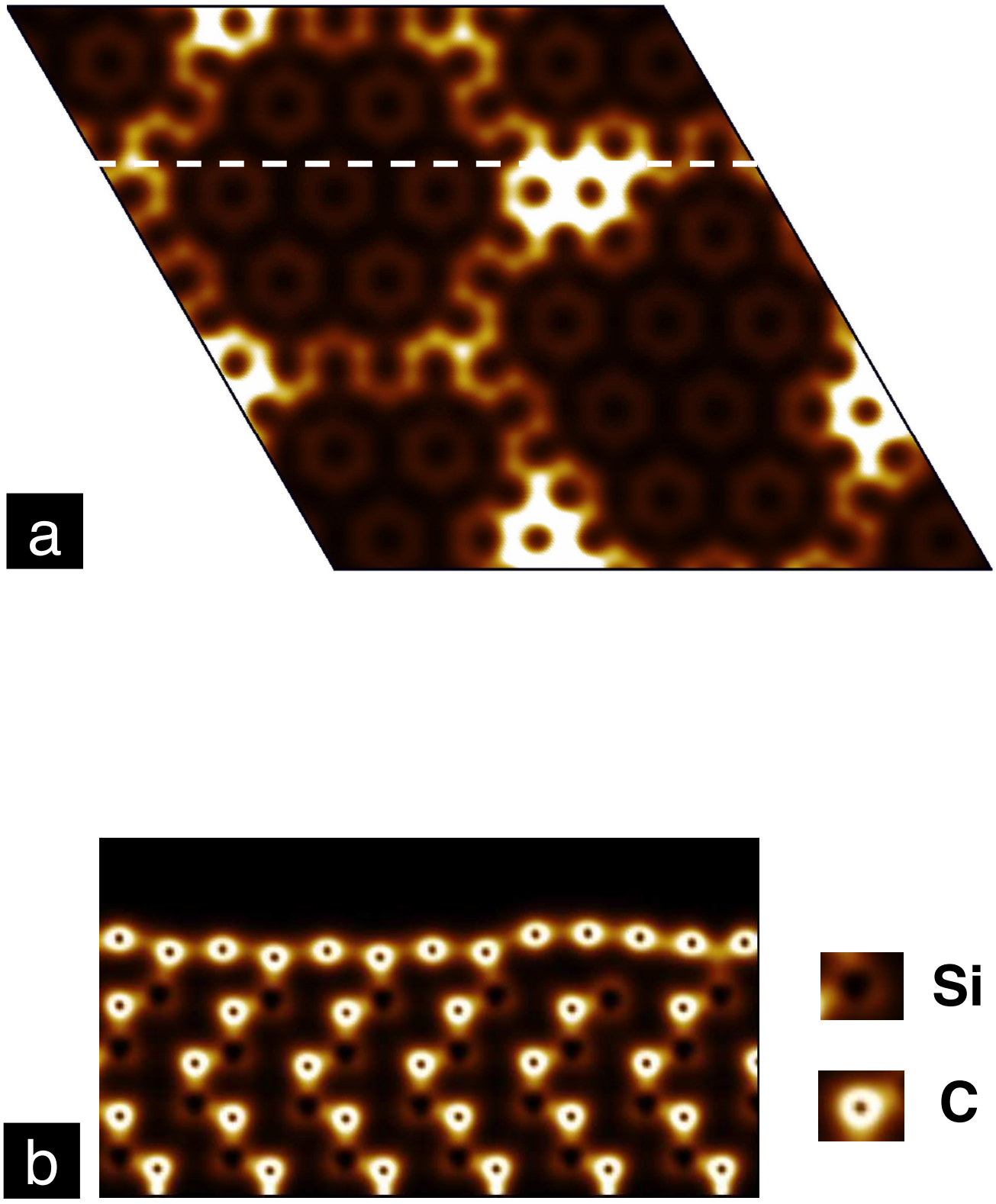

Figure 2

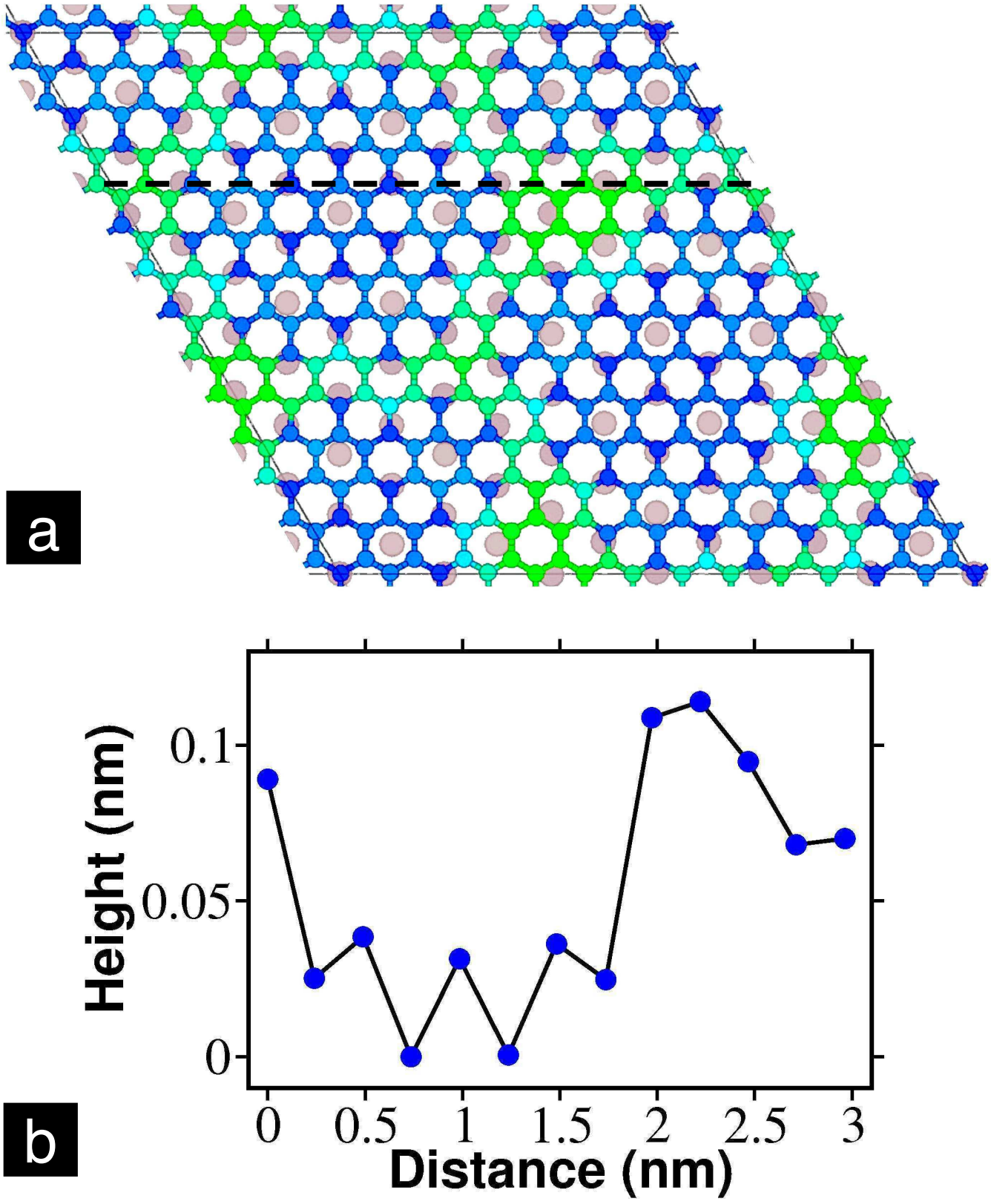

Figure 3

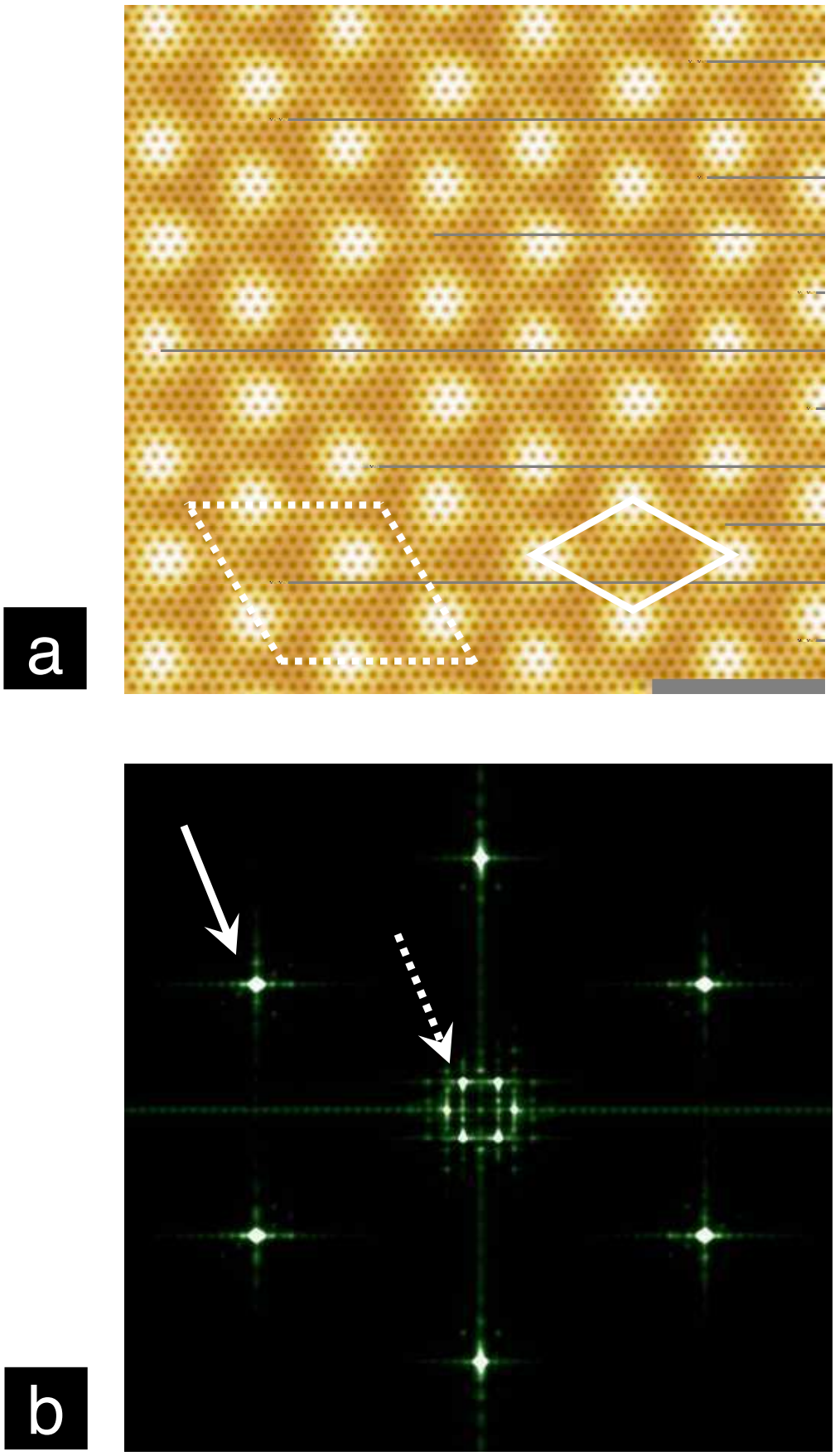

Figure 4

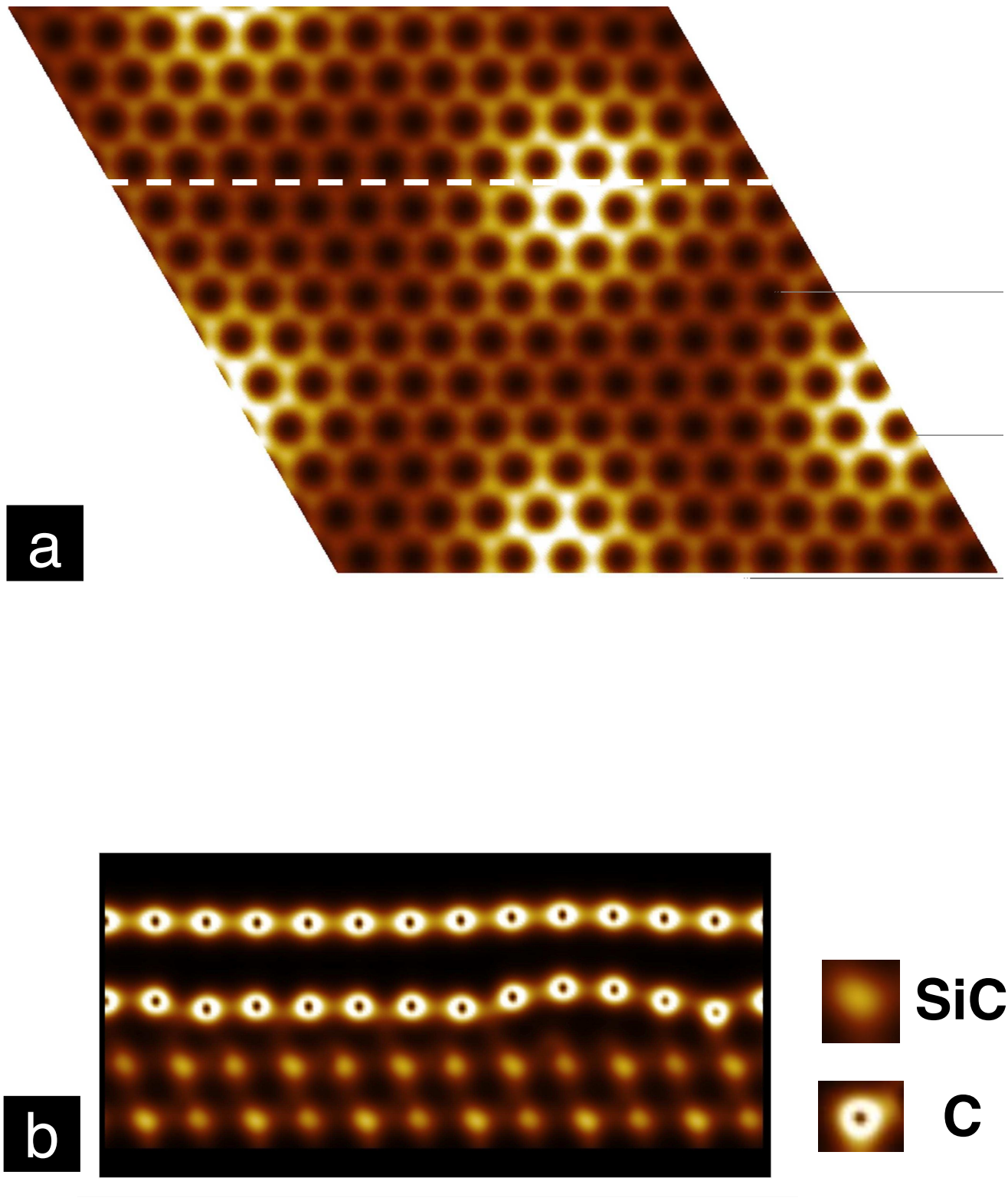

Figure 5

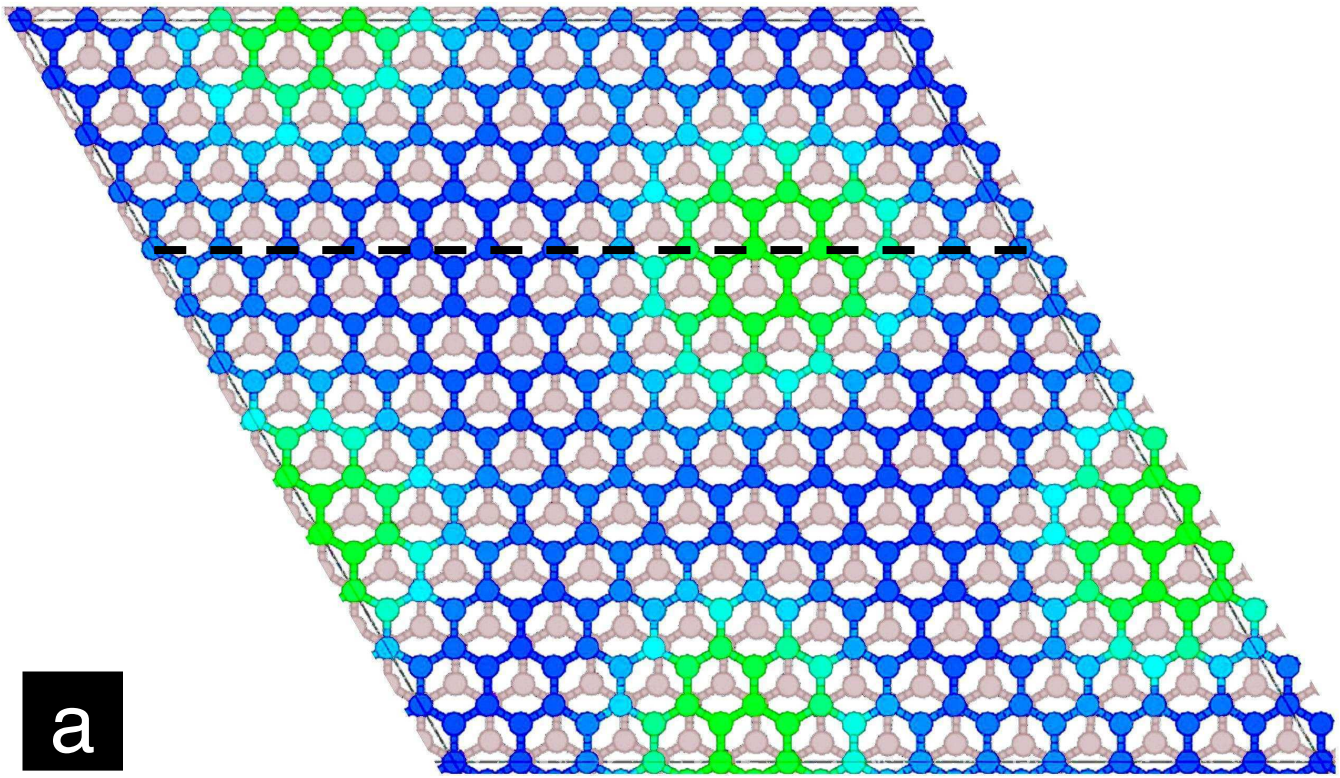

a

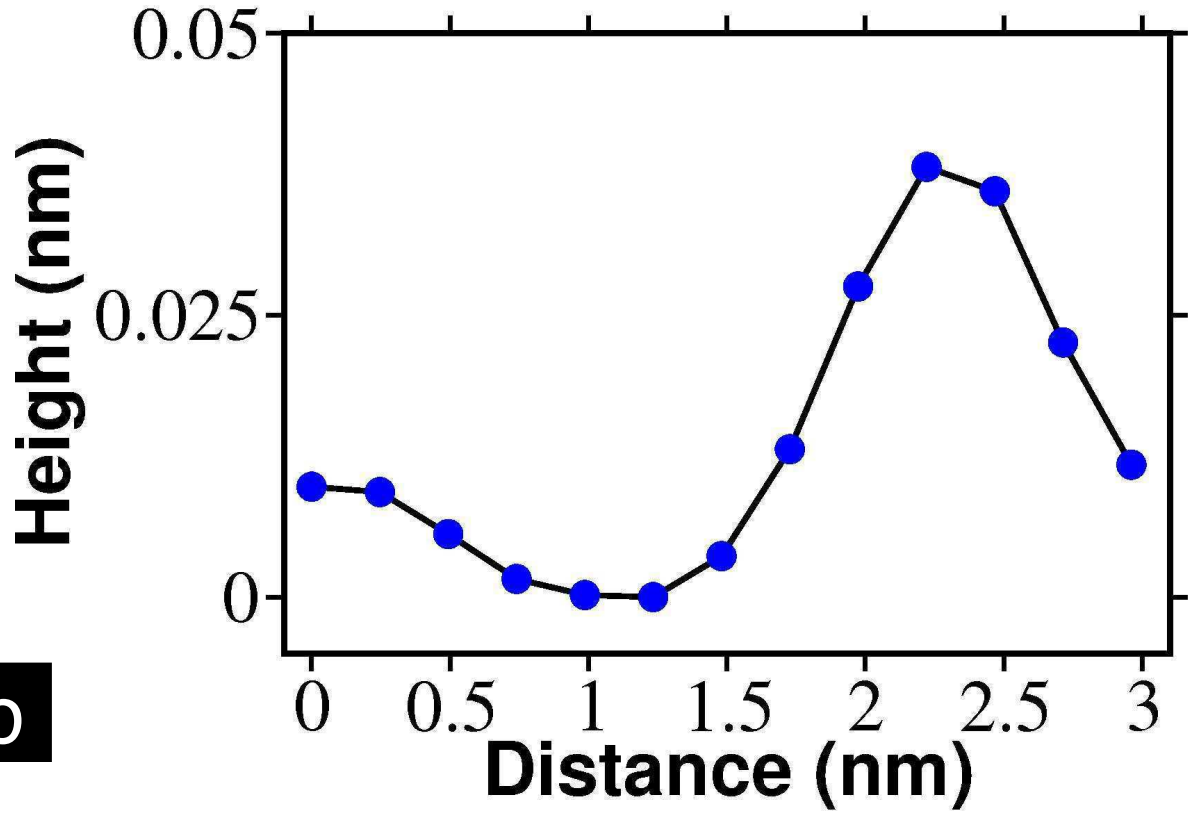

b

Figure 6

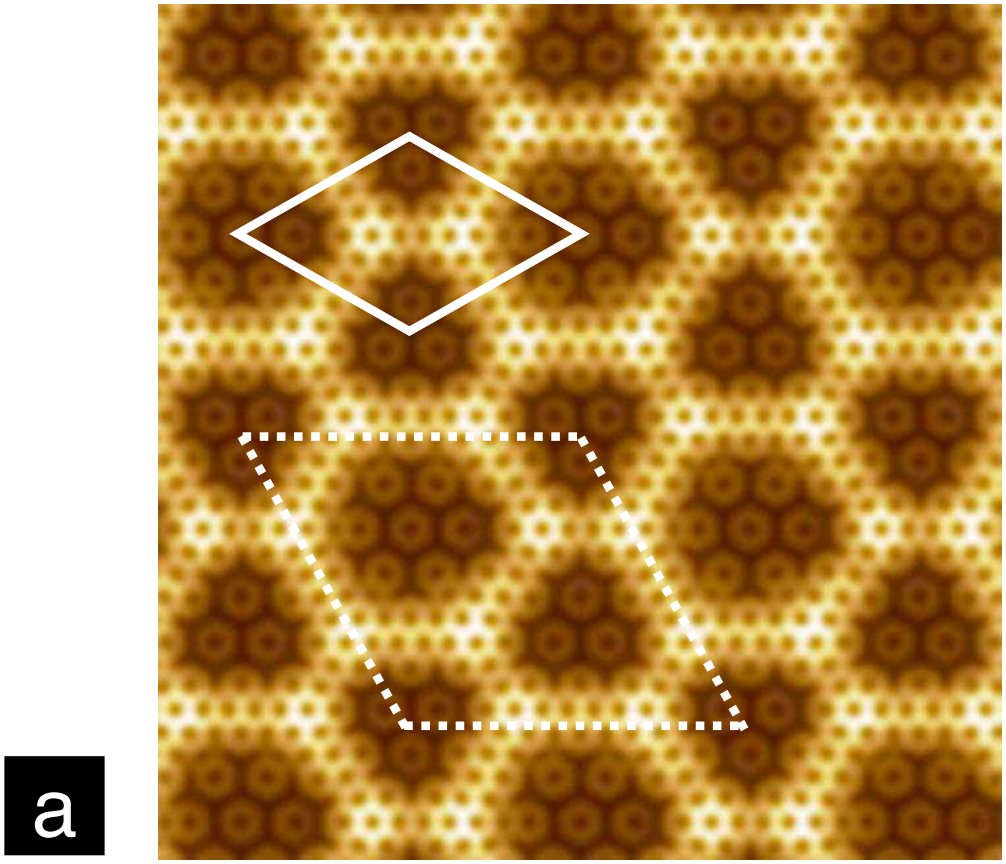

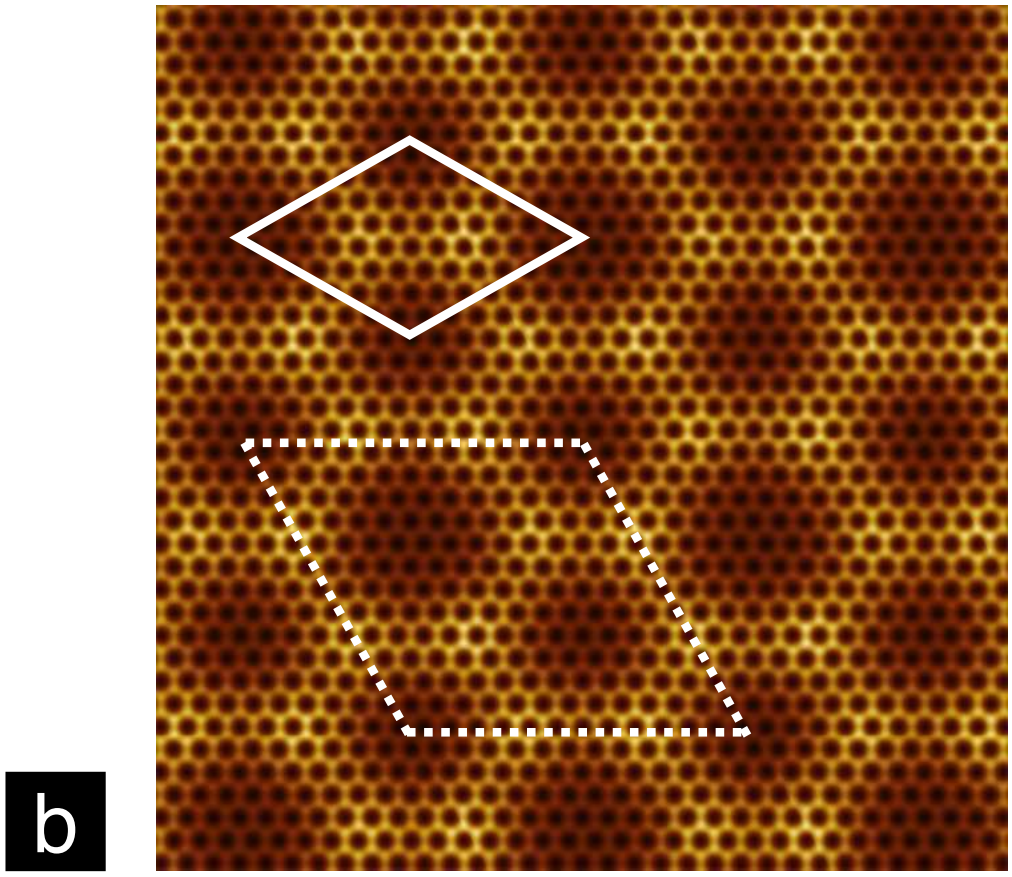

Figure 7

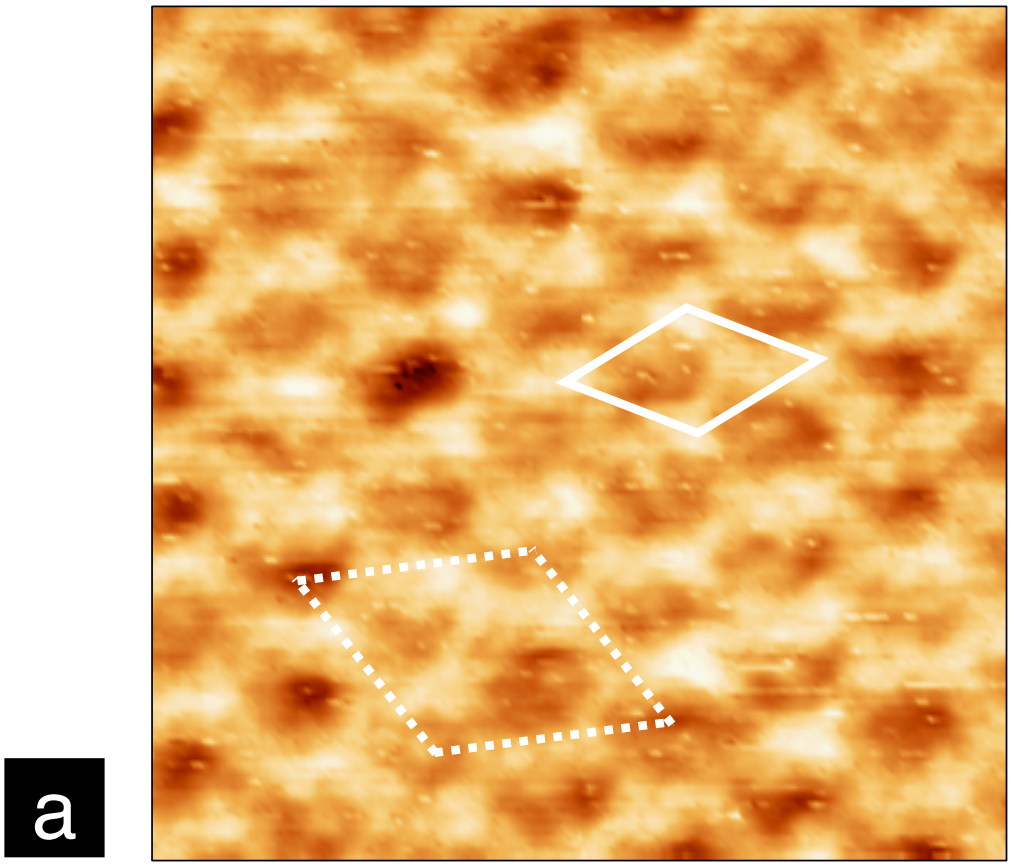

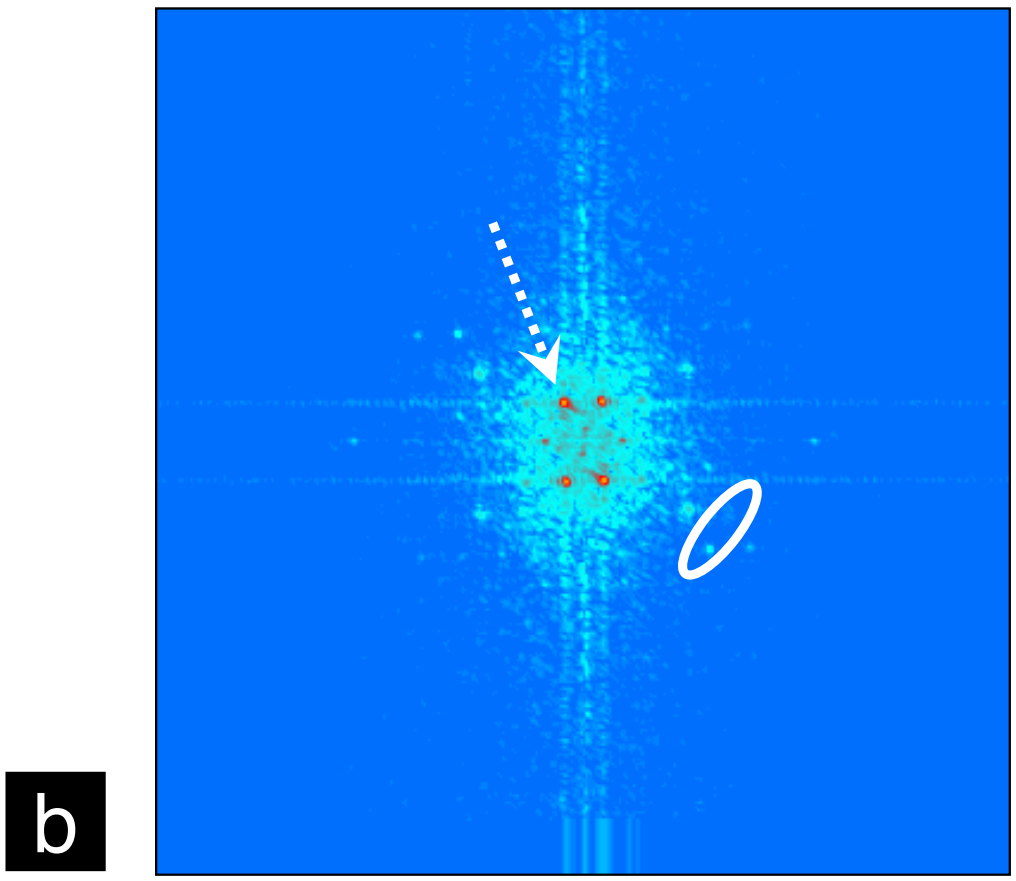

Figure 8

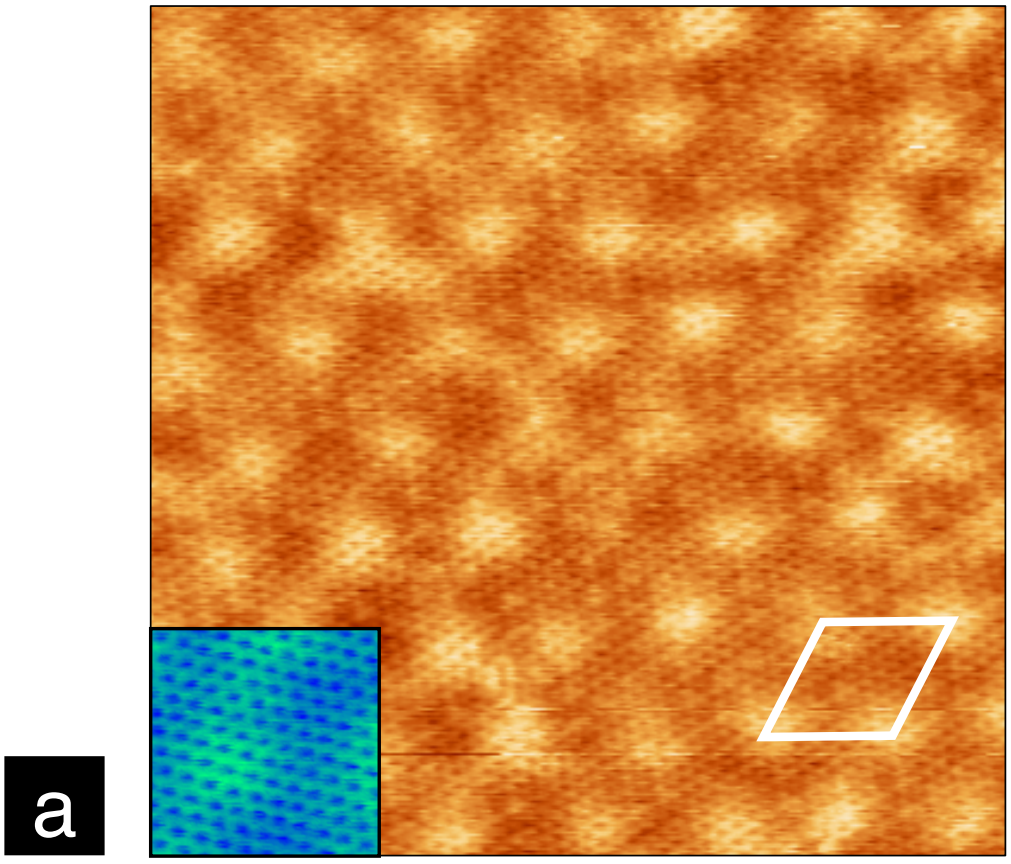

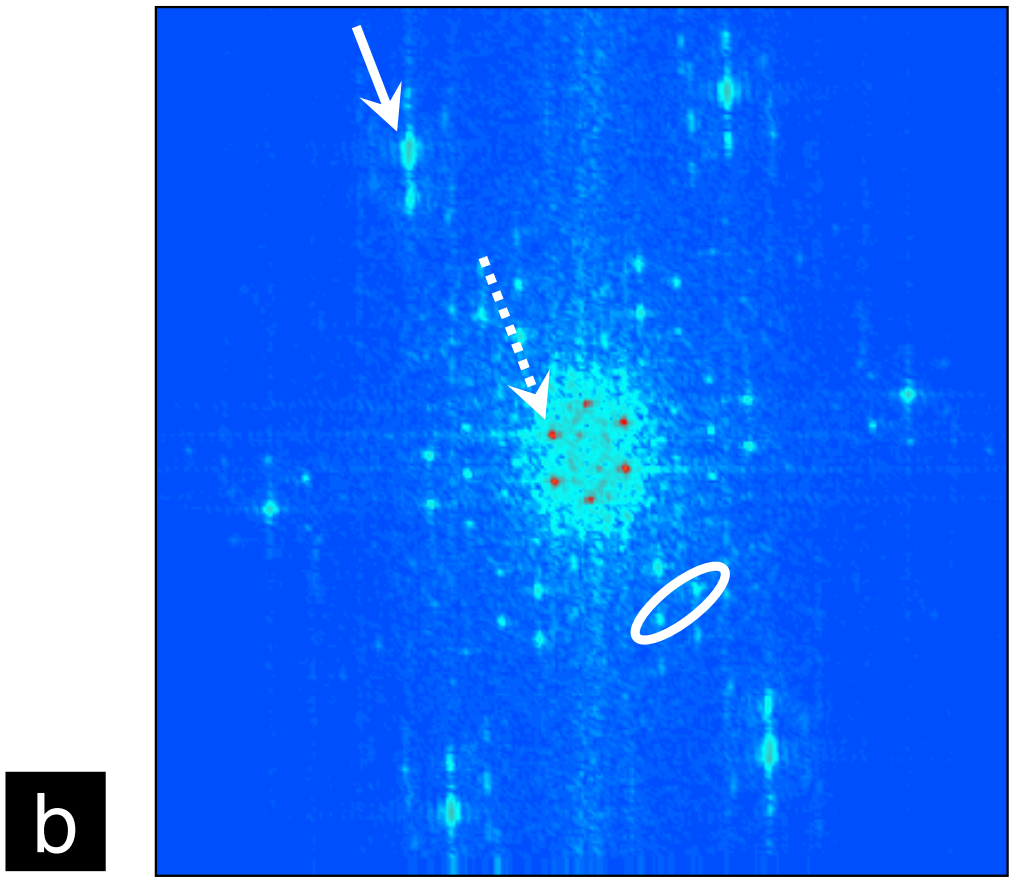

Figure 9